AIAA JOURNAL
Vol. 43, No. 3, March 2005

Intelligent Genetic Algorithm and Its Application to Aerodynamic Optimization of Airplanes

Jenn-Long Liu*
Leader University, Tainan 709, Taiwan, Republic of China

A new genetic algorithm (GA), called intelligent GA, is proposed by the inclusion of a fractional factorial design in the crossover operator to determine the best combination of design variables. That is, in the proposed GA, the chromosomes of children are generated via an intelligent crossover process with factorial experiments after completing the selection of GA operators. This gene mating process differs from the traditional GA, where the child chromosome is generally generated via randomization. Accordingly, the traditional GA incorporating the technique of fractional factorial design into the crossover operator markedly enhances the performance in terms of evolutionary efficiency. Another GA, called Taguchi-GA, that incorporates the Taguchi orthogonal arrays into the crossover operator is also developed to compare the performance of the presented intelligent GA. Four representative test cases, including two multimodal functions, a nonlinear dynamic control function, and a profile fitting of a high lift airfoil are performed via the traditional GA, micro-GA, Taguchi-GA, and present GA to assess the capacity and efficiency of the proposed GA. The computational solutions of the convergence history and optimal objective function for the test cases demonstrate that the proposed intelligent GA outperforms the other three GAs. Moreover, the presented new intelligent GA and the other three GAs are applied to the aerodynamic optimization of two airplanes, namely, an advanced defense airplane and an F-16A fighter. The redesigned wing planform is obtained by computations made with an aerodynamic flow solver, and the present GA depicts the optimal swept angle, aspect ratio, and taper ratio. The drag distribution and convergence history show that the proposed intelligent GA has a high evolutionary efficiency when applied to practical engineering problems.

Introduction

GENETIC algorithms (GAs) have emerged as handy tools in a wide range of application areas, such as medicine, image processing, laser technology, aeronautics, artificial neural networks, control, robotics, and so on.[1] Coley also pointed out that the number of published papers annually that discuss GAs has grown rapidly during recent decades. Basically, a GA uses the probabilistic transition and nondeterministic rules using selection, crossover, and mutation operators to search possible solution spaces.[2,3] Among the three operations, the crossover operator is the major operator involved with the evolutionary efficiency of GA. Generally, a traditional GA, such as simple GA,[2] is capable of achieving a near global optimum, but it usually requires large population sizes and generations for evolution, such that the GA is inefficient in practical engineering applications.[4] Therefore, many works combined the GA with different approaches, for example, hybrid searching,[4] the single- or multisimplex method,[5] simulated annealing,[6,7] Tabu search (see Ref. 8), and design of experiment (DOE)[9] to improve the evolutionary efficiency. Ho et al.[9] incorporated the well-known orthogonal arrays (OA) of Taguchi into the crossover operator to create better chromosomes of children based on those of parents through several factorial experiments, rather than exchanging genes randomly. Their strategy resulted in a remarkable improvement in the search ability of GA.

During the past few decades, several approaches based on DOE have been applied to quality management in industrial engineering.[10] Among these approaches, three are particularly well known, namely, the classical, Taguchi, and Shainin. The principal techniques of the classical approach begin with fractional factorials that are derived from full factorial factors and end with evolutionary optimization. The Taguchi method uses OAs in tolerance design and employs analysis of variance and signal-to-noise for statistical evaluation (see Ref. 11). Moreover, the Shainin method reduces the number of design variables from large numbers, for example, 20–100, to small numbers, for example, 4 or fewer; this method then implements factor analysis with full factorial orthogonal tables (see Ref. 12). All three approaches are far superior to conventional statistical process control, which can be used to solve chronic problems by the use of control charts. In the GA calculation, the number of design variables ("factors" in the DOE) is kept constant throughout the iterative process. Accordingly, the Shainin method cannot be directly applied to the GA, although it effectively reduces variations and reliably generates optimal results. Moreover, Bhote reported that "the confounding with multiple aliases (false names) of interaction effects with main effects, caused by highly saturated experimental designs, makes the fractional factorial statistically weak and the Taguchi orthogonal array even weaker,"[10] Bhote, thus, emphasized that full factor analysis is the most reliable means of achieving optimal design. Bhote also mentioned that classical fractional factorial analysis with evolutionary optimization is superior to the Taguchi method. The practical computations associated with full factor analysis are expensive and cannot be undertaken for large parameter optimization problems involving numerous design variables; the method of fractional factorial analysis appears to be a good alternative for analyzing the main factor effects. Consequently, this study proposes an intelligent GA by incorporation of the fractional factorial design (FFD) into the crossover operator of GA to enhance the numerical efficiency for solving global optimization problems.

The efficiency of the proposed intelligent GA is evaluated by comparing the computational results that use this method with those obtained by the traditional GA, micro-GA, and Taguchi-GA. In this work, the four GAs are all binary encoded. The methodology of the traditional GA employed here includes a tournament selection,[13] uniform crossover, jump mutation, and elitist strategy. Additionally, the micro-GA, proposed by Krishnakumar,[14] is presented for comparing the evolutionary efficiency. The micro-GA avoids premature convergence and improves the convergence rate for many multimodal problems. As mentioned in Ref. 15, the mutation operation can be skipped when the micro-GA of Krishnkumar is used. The methodology of the proposed intelligent GA and Taguchi-GA

Received 15 December 2003; revision received 29 August 2004; accepted for publication 15 September 2004. Copyright © 2004 by the American Institute of Aeronautics and Astronautics, Inc. All rights reserved. Copies of this paper may be made for personal or internal use, on condition that the copier pay the $10.00 per-copy fee to the Copyright Clearance Center, Inc., 222 Rosewood Drive, Danvers, MA 01923; include the code 0001-1452/05 $10.00 in correspondence with the CCC.

*Associate Professor, Department of Information Management; jlliu@mail.leader.edu.tw. Member AIAA.

uses the tournament selection, intelligent crossover, jump mutation operations, and elitist strategy. Moreover, the intelligent crossover operation for the proposed GA incorporates the FFD, whereas the Taguchi-GA incorporates the Taguchi OA. The subsequent section decribes the numerical procedures of the proposed intelligent GA and the Taguchi-GA.

In aerodynamic applications, many numerical approaches have been applied to the airfoil, wing, and aircraft designs.[16–20] Among these optimization algorithms, heuristic-based soft computing methods have proven relatively powerful in the applications of airfoil and wing designs. A clear advantage of soft computing is that the search does not require the computation of gradients. Therefore, the use of the GA as a design tool appears to be a good option for analyzing aerodynamic problems as long as the major weakness of GAs in evolutionary efficiency can be improved. Accordingly, this work develops the new intelligent GA that is suitable for application to complex aerodynamic designs due to its high computing efficiency. First, several test cases are performed to assess the efficiency and capacity of the presented intelligent GA. These cases include two multimodal functions, a nonlinear dynamic control function, and a profile fitting of a high-lift LS(1)-0417 modified airfoil. Furthermore, the presented GA is applied to the aerodynamic optimizations to redesign the wing planforms of an advanced defense airplane and an F-16A fighter.

Construction of the Presented Intelligent GA

Description of an Objective Function

The general form of an objective function with the variable vector $\boldsymbol{x}$ is expressed as $F(\boldsymbol{x})$. The variable $\boldsymbol{x}$ represents the solution vector with N_{dim} variables and is defined as a set $\{x_i, i = 1, N_{\text{dim}}\}$. In the GA computation, each variable x_i represents the genes of an individual, and vector $\boldsymbol{x}$ represents a complete chromosome. Each of the individuals is assigned a fitness value based on the calculation of objective function $F(\boldsymbol{x})$. The variables in most of the optimization problems are subject to the range and linear/nonlinear constraints.

Pseudocode of Proposed Intelligent GA

```
Begin
Create initial chromosomes of population randomly; /* BINARY
   ENCODING */
Construct a two-level orthogonal table based on classical
   fractional factorials;
Do {
   design variables = DECODE(chromosomes);
   fitness = EVAL(objective function)
   parents = SELECT(individuals of population);
      /* TOURNAMENT SELECTION */
   children = FFD(parent1, parent2); /* INTELLIGENT
      CROSSOVER */
   new children = MUTAT (children); /* JUMP MUTATION */
   best children = ELITISM (new children); /* ELITIST
      STRATEGY */
   } While (stopping criterion is not satisfied);
End
```

Intelligent Crossover Operator with FFD

After the tournament selection operator is completed,[13] this study applies FFD, rather than one-point, multipoint, or uniform crossover to implement the crossover operator. The basic FFD used in this work is based on classical factorial analysis with two-level, multivariable orthogonal tables.[10] Applying the fractional factorial analysis to the crossover operator yields an arrangement of two-level factors that correspond to the levels of the design variables of selected parents. In the classical factorial experiments, the two levels are labeled by $-$ and $+$. Hence, x_i^- and x_i^+ represent the two levels of the design variable x_i in this work. That is, x_i^- is the level value of parent 1, whereas x_i^+ is the level value of parent 2. Table 1 lists the level distribution of seven factors A, B, ..., and ABC, each comprising two levels.[10] Table 2 lists the Taguchi OA level distribution of seven factor numbers, also comprising two levels. Table 1 shows that the experiment retains the balance of a western experiment design. Each column has the same amount of levels $-$ and $+$. The numerical procedure steps for the fractional factorial analysis are as follows:

1) First, if N_{dim} factors (named by design variables in the GA) each have two levels, then build a table containing m rows and $m-1$ columns. The value m is defined with the integer $2^{[\log_2(N_{\text{dim}}+1)]}$. For example, if seven factors ($N_{\text{dim}} = 7$) are associated with vector $\boldsymbol{x}$, then eight experiments ($m = 8$) are conducted for factorial analysis. Table 1 shows that levels $-$ and $+$ in columns A, B, and C are assigned to each cell position regularly, based on the classical full factorial design principle.[10] In columns AB, AC, BC, and ABC, each cell level is determined via the inner products of columns A and B; A and C; B and C; and A, B, and C.

2) The first experiment has one factor set to $\boldsymbol{x} = \{x_1^-, x_2^-, x_3^+, x_4^-, x_5^+, x_6^+, x_7\}$, which is obtained by combining the factors from A to

Table 1 Orthogonal table of FFD with seven two-level factors

	Factor label and design variable							
Experiment	A, $x_1^{\pm}$	B, $x_2^{\pm}$	AB, $x_3^{\pm}$	C, $x_4^{\pm}$	AC, $x_5^{\pm}$	BC, $x_6^{\pm}$	ABC, $x_7^{\pm}$	Output
1	$-$	$-$	$+$	$-$	$+$	$+$	$-$	F_1
2	$+$	$-$	$-$	$-$	$-$	$+$	$+$	F_2
3	$-$	$+$	$-$	$-$	$+$	$-$	$+$	F_3
4	$+$	$+$	$+$	$-$	$-$	$-$	$-$	F_4
5	$-$	$-$	$+$	$+$	$-$	$-$	$+$	F_5
6	$+$	$-$	$-$	$+$	$+$	$-$	$-$	F_6
7	$-$	$+$	$-$	$+$	$-$	$+$	$-$	F_7
8	$+$	$+$	$+$	$+$	$+$	$+$	$+$	F_8

Table 2 Orthogonal table of Taguchi OA with seven two-level factors

	Factor no. and design variable							
Experiment	1, $x_1^{1,2}$	2, $x_2^{1,2}$	3, $x_3^{1,2}$	4, $x_4^{1,2}$	5, $x_5^{1,2}$	6, $x_6^{1,2}$	7, $x_7^{1,2}$	Output
1	1	1	1	1	1	1	1	F_1
2	1	1	1	2	2	2	2	F_2
3	1	2	2	1	1	2	2	F_3
4	1	2	2	2	2	1	1	F_4
5	2	1	2	1	2	1	2	F_5
6	2	1	2	2	1	2	1	F_6
7	2	2	1	1	2	2	1	F_7
8	2	2	1	2	1	1	2	F_8

Table 3 Fractional factorial analyses with the FFD

Experiment	Factor label and design variables: A, $x_1^- = -5.0$, $x_1^+ = 4.0$	B, $x_2^- = 8.5$, $x_2^+ = 2.0$	AB, $x_3^- = 6.0$, $x_3^+ = -4.0$	C, $x_4^- = -5.5$, $x_4^+ = 4.5$	AC, $x_5^- = 8.0$, $x_5^+ = 5.0$	BC, $x_6^- = -2.0$, $x_6^+ = 3.0$	ABC, $x_7^- = 9.0$, $x_7^+ = -1.0$	Output
1	−5.0	8.5	−4.0	−5.5	5.0	3.0	9.0	−1.43
2	4.0	8.5	6.0	−5.5	8.0	3.0	−1.0	10.02
3	−5.0	2.0	6.0	−5.5	5.0	−2.0	−1.0	−0.94
4	4.0	2.0	−4.0	−5.5	8.0	−2.0	9.0	−0.20
5	−5.0	8.5	−4.0	4.5	8.0	−2.0	−1.0	−2.18
6	4.0	8.5	6.0	4.5	5.0	−2.0	9.0	16.44
7	−5.0	2.0	6.0	4.5	8.0	3.0	9.0	12.40
8	4.0	2.0	−4.0	4.5	5.0	3.0	−1.0	11.86
Contribution	30.28	0.28	−29.86	31.07	5.88	19.75	−8.45	
Selected level	+	+	−	+	+	+	−	
Best factor	4.0	2.0	6.0	4.5	5.0	3.0	9.0	21.44
Next best	4.0	8.5	6.0	4.5	5.0	3.0	9.0	21.37

ABC with the assigned levels. In the following, its function value f_1 is computed and placed in the first position of the column "Output." The computations then are repeated for the remaining seven experiments with function values $f_2, f_3, \ldots,$ and f_8. Then the eight experiments are finished.

3) In column A, multiply the function values $f_2, f_3, \ldots,$ and f_8 by the corresponding algebraic value −1 for level − and 1 for level +. The effect of factor A on the level is determined by adding the eight products together. The mathematical form for each factor i is

$$C_i = \sum_{j=1}^{8} N_{i,j} \times f_j$$

In this situation, $N_{i,j}$ equals −1 when the cell is at level −, and equals 1 when it is at level +. The summation C_1 is positioned first in the row "Contribution" (Table 3), and is associated with factor A. The multiplication and summation operations are completed for the remaining six values, $C_2, C_3, \ldots,$ and C_7, and placed in the second, third, . . . , and seventh positions in the row Contribution; the effects of factors B, C, . . . , and ABC on the levels are thus obtained.

4) Check the signs of the seven values $C_1, C_2, \ldots,$ and C_7 listed in the row Contribution; if C_i is negative, then place the symbol − in the row "Selected Level" in Table 3. Otherwise, select symbol +. The dominant levels of the seven factors can thus be determined.

5) The best combination of x_i^{best} for the seven factors is determined from the factors with selected levels, listed in the row Best Factor in Table 3, and the best value of the function is obtained by calculating the objective function $f(\boldsymbol{x}_i^{\text{best}})$. The choice principle for each best factor $\boldsymbol{x}_i^{\text{best}}$ is expressed as follows:

$$x_i^{\text{best}} = \begin{cases} x_i^-, & \text{if} \quad \text{sign}(C_i) < 0 \\ x_i^+, & \text{if} \quad \text{sign}(C_i) > 0 \end{cases} \tag{1}$$

6) To promote numerical computation efficiency, this study employs the strategy of two children per pair of parents. The second child is created initially by replicating the factors from the first child and, afterward, by replacing the level factor with another one at the position of minimal absolute value of contribution. By the use of the strategy of two children per pair of parents, the proposed strategy only requires one-half of the CPU time of the strategy of one child per pair of parents.

Illustration of the Use of FFD

This work evaluates a multimodal function for demonstrating the numerical procedure of FFD to clarify the effectiveness of the FFD technique in generating the best design variables to the crossover operator of GA. The objective function is as follows:

$$\begin{aligned} \text{maximize} \qquad & F(\boldsymbol{x}) = \sum_{i=1}^{N_{\text{dim}}} \left[x_i \sin\left(\sqrt{|x_i|}\right) \right] \\ \text{subject to} \qquad & x_i \in [-10, 10] \end{aligned} \tag{2}$$

When the number of dimensions N_{dim} equals seven, the multimodal function has a maximum value of $F(\boldsymbol{x}_i^{\text{best}}) = 26.717$ at $\boldsymbol{x}^{\text{best}} = 5.2392$. Table 3 lists the setting of the design variable for the + and − levels, which are {−5.0, 8.5, 6.0, −5.5, 8.0, −2.0, 9.0} and {4.0, 2.0, −4.0, 4.5, 5.0, 3.0, −1.0}, respectively. These values are selected randomly from within the range [−10,10]. Accordingly, the functional values of the current and probed states equal 0.95 and 9.76 by the use of Eq. (2). Eight function values, −0.41, 8.25, . . . , and 9.75, listed in column Output, are obtained by computing Eq. (2) with eight design variable sets {−5.0, 8.5, −4.0, −5.5, 5.0, 3.0, 9.0}, {4.0, 8.5, 6.0, −5.5, 8.0, 3.0, −1.0}, . . . , and {4.0, 2.0, −4.0, 4.5, 5.0, 3.0, −1.0}. The value of each factor, listed in the row Contribution, is obtained with

$$C_i = \sum_{j=1}^{8} N_{i,j} \times f_j$$

Accordingly, the contributions of factors A to ABC are computed as −1.43, 10.02, . . . , and 11.86. The signs of the contributions show that the dominant levels of the factors A, B, and ABC are +, +, . . . , −. Therefore, the best factors are selected as {4.0, 2.0, 6.0, 4.5, 5.0, 3.0, 9.0}, and their functional value increases markedly to 21.44. The result is notable for creating a good child from the crossover operation. Additionally, the second child is easily generated by changing the factor value of 2.0 to 8.5 at the position of the minimal absolute value of Contribution. The function fitness of the second child equals 21.37. The high fitness value is clearly maintained for the second child. Accordingly, FFD is shown to be effective for determining a good combination of design variables.

Similarly, the computed result by the use of factorials analysis via the Taguchi OA (see Ref. 11) listed in Table 2, is shown in Table 4. The variables S_{j1} and S_{j2} denote the main effects of factor j at levels 1 and 2.

$$S_{jk} = \sum_{i=1}^{8} F_i^2 \times C_{j,k}, \qquad k = 1, 2 \tag{3}$$

The coefficient $C_{j,k}$ is set to one when the level value (1 or 2) of factor j in the ith experiment is identical; otherwise, it is set to zero. The main effect difference (MED) represents the value of difference between the terms S_{i1} and S_{i2}. Check the signs of the seven values of MED; if MED is negative, then place the symbol 1 in the row "Selected Level" (Table 4), otherwise, select symbol 2. The dominant levels of the seven factors are thus determined. Table 4 shows that the best factors for the first child are determined to be {4.0, 2.0, 6.0, 4.5, 8.0, 3.0, 9.0} with fitness 19.97. Moreover, the fitness value of the second child drops to 17.86 when the factor value changes from 9.0 to −1.0 at the position of the minimal absolute value of MED. Clearly, the illustrated result shows that the presented intelligent GA using FFD is superior to that using Taguchi OA.

Table 4 Fractional factorial analysis with Taguchi OA

Experiment	Factor no. and design variables: 1, $x_1^1=-5.0$, $x_1^2=4.0$	2, $x_2^1=8.5$, $x_2^2=2.0$	3, $x_3^1=6.0$, $x_3^2=-4.0$	4, $x_4^1=-5.5$, $x_4^2=4.5$	5, $x_5^1=8.0$, $x_5^2=5.0$	6, $x_6^1=-2.0$, $x_6^2=3.0$	7, $x_7^1=9.0$, $x_7^2=-1.0$	Output
1	−5.0	8.5	6.0	−5.5	8.0	−2.0	9.0	−0.37
2	−5.0	8.5	6.0	4.5	5.0	3.0	−1.0	11.69
3	−5.0	2.0	−4.0	−5.5	8.0	3.0	−1.0	−4.94
4	−5.0	2.0	−4.0	4.5	5.0	−2.0	9.0	1.47
5	4.0	8.5	−4.0	−5.5	5.0	−2.0	−1.0	−0.91
6	4.0	8.5	−4.0	4.5	8.0	3.0	9.0	12.44
7	4.0	2.0	6.0	−5.5	5.0	3.0	9.0	13.67
8	4.0	2.0	6.0	4.5	8.0	−2.0	−1.0	12.92
S_{i1}	163	292	490	212	346	170	344	
S_{i2}	509	380	182	460	326	502	328	
MED	−346	−88	308	−248	19	−332	15	
Selected level	2	2	1	2	1	2	1	
Best factor	4.0	2.0	6.0	4.5	8.0	3.0	9.0	19.97
Next best	4.0	2.0	6.0	4.5	8.0	3.0	−1.0	17.86

Results and Discussion

This work proposes several benchmarking test cases for finding the global optima to investigate the computational performances of the presented intelligent GA. The traditional GA, micro-GA, and Taguchi-GA are also performed to provide a comparison. The parameter settings in all cases for crossover and mutation probabilities (p_c and p_m) equal 0.5 and 0.02, respectively. This work employs a binary vector as a chromosome for representing real values of the variable vector $\boldsymbol{x}$. The binary-encoded length is set to at least 22 for each real design variable to achieve the required precision of six places after the decimal point. The maximum value of the population size used in this work ranges from 6 to 30, depending on the number of design variables involved in the problems. The population size used for each case is indicated in the figure of convergency history. Notably, the main difference among the traditional GA, Taguchi-GA, and presented GA lies in the crossover operator. The traditional GA uses uniform crossover, whereas the Taguchi-GA and proposed intelligent GA use Taguchi OA and FFD, respectively, to generate good variables through fractional factorials. The test cases include two multimodal functions, a nonlinear dynamic control function, and a profile fitting of a high-lift LS(1)-0417 modified airfoil. Furthermore, the proposed intelligent GA is applied to the aerodynamic optimization to optimize the airplane wing planform to evaluate the algorithmic abilities and efficiencies in practical engineering design. Additionally, all of the preceding cases obtained with the four GAs are repeatable.

First Multimodal Function

The first multimodal function includes two variables x_1 and x_2. Moreover, the function and range of the design variables are as follows[21]:

$$\text{maximize} \qquad F(x_1, x_2) = \prod_{i=1}^{2} \{\sin^6(5.1\pi\, x_i + 0.5) \times \exp[-4\,\ell_n 2(x_i - 0.0667)^2/0.64]\}$$

$$\text{subject to} \qquad -1 \le x_i \le 1, \qquad i = 1, 2 \tag{4}$$

The global maximum of the function equals one at $\boldsymbol{x}^* = 0.06683$. Figure 1a shows the contours of the function values and reveals that the objective function has many local optima with a unique global maximum in the domain $[-1, 1]$. Figure 1b shows the presented intelligent GA, Taguchi-GA, micro-GA, and traditional GA, along with the convergence histories of function evaluation. Figure 1b shows that the proposed GA and Taguchi-GA perform excellently in achieving the global optimum, whereas the micro-GA and traditional GA are slow to achieve global maximization. Additionally, the micro-GA outperforms the traditional GA in this case.

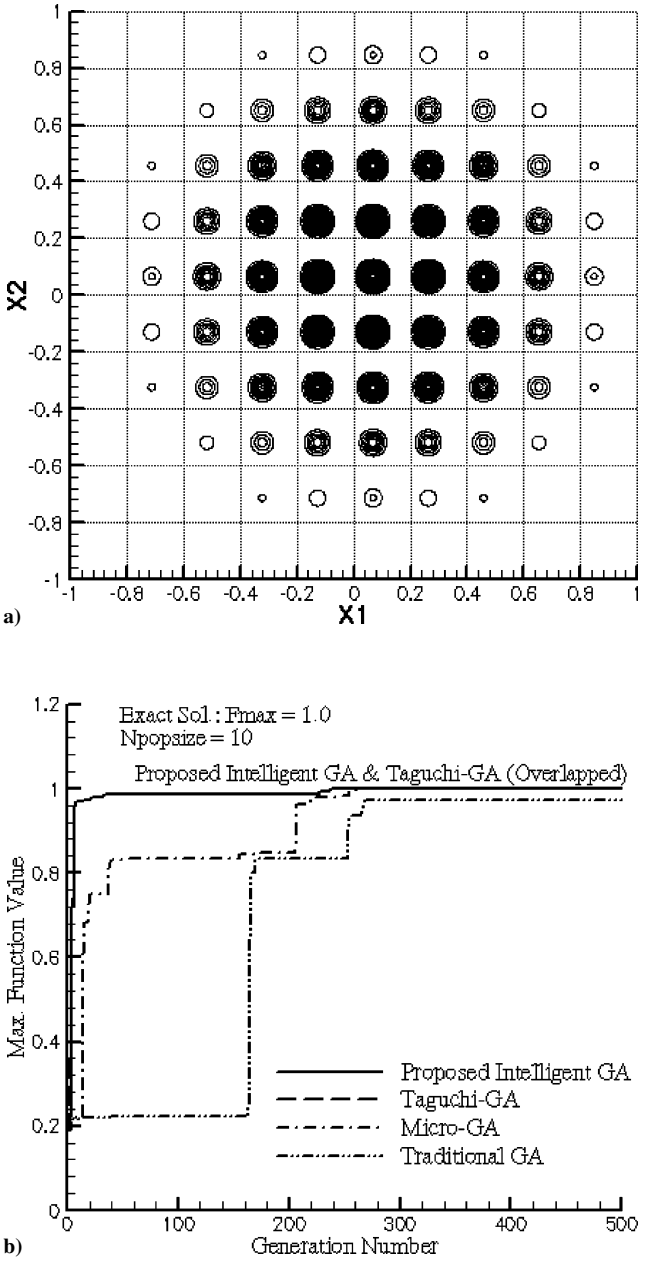

Fig. 1 Use of the traditional GA, micro-GA, Taguchi-GA, and proposed intelligent GA to solve te first multimodal function: a) contours of function value and b) convergence histories and optimal solutions.

Second Multimodal Function

This case, which involves the evaluation of the proposed intelligent GA, represents a difficult problem for determining the global optimum for a large number of dimensions N_{dim}. The objective function is a combination of two sinusoidal functions, as follows:

$$\text{maximize} \qquad F(\boldsymbol{x}) = a\prod_{i=1}^{N_{\text{dim}}}\sin(x_i) + \prod_{i=1}^{N_{\text{dim}}}\sin(5x_i)$$

$$\text{subject to} \qquad -5 \le x_i \le 5 \tag{5}$$

The parameters a and N_{dim} dominate the peaks and slopes of the multimodal function. The global optimum is $(1+a)$ at position $\boldsymbol{x}^* = \pi/2$; this optimum is surrounded by various local optima that are the mathematical roots of both sinusoidal functions, $\sin x = 1$ and $\sin 5x = 1$. This work sets the coefficient a to 0.5 and the two values of N_{dim} to 20 and 40. In this case, the population size and maximum generation number equal 20 and 10,000 for GA computation. Figure 2a shows that the proposed intelligent GA and Taguchi-GA reached the global optima at 857 and 1409 generations. Moreover, both the micro-GA and traditional GA have difficulty in reaching the global solution after 10,000 generations. In this case, the proposed intelligent GA exhibits the best convergence rate. When N_{dim} increases to 40, the two intelligence algorithms can still quickly achieve the global optimum, whereas the convergence rates of the traditional GA and micro-GA become quite slow (Fig. 2b). Figure 2b also shows that the presented GA achieves the best performance. Generally, the solution of the multimodal function N_{popsize} and generation require large values. In the present calculations, the value N_{popsize} is specified to 20 only.

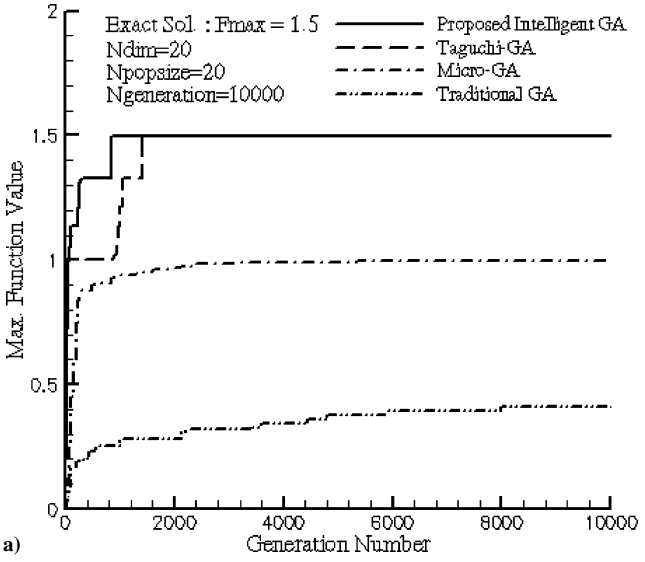

a)

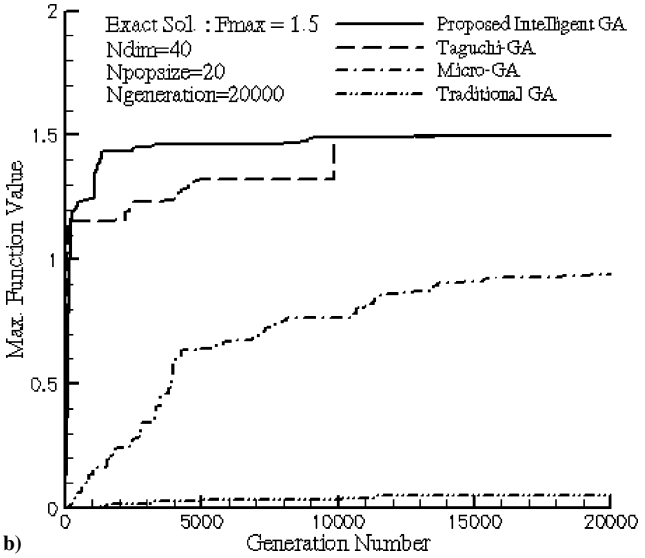

b)

Fig. 2 Convergence histories and optimal solutions obtained with the traditional GA, micro-GA, Taguchi-GA, and proposed intelligent GA to solve the second multimodal function with a) $N_{\text{dim}} = 20$ and b) $N_{\text{dim}} = 40$.

Nonlinear Dynamic Control Function

This problem involves minimizing a dynamic control function. The case calculation further examines the minimum optimization and convergence of the four GAs. The nonlinear function is formulated as follows[22]:

$$\text{minimize} \qquad F(\boldsymbol{x}) = \left(x_{N_{\text{dim}}}^2 + \sum_{k=0}^{N_{\text{dim}}-1}\left(x_k^2 + u_k^2\right)\right)$$

$$\text{subject to} \qquad x_{k+1} = x_k + u_k, \qquad k = 0, 1, \ldots, N_{\text{dim}} - 1 \tag{6}$$

The parameter x_0 presented in Eq. (6) is an initial state, and its value is set to 10.0 here. The range constraints are chosen from within the interval $[-10, 10]$ for each design variable. Moreover, the optimal solution can be analytically expressed as $J^* = K_0 x_0^2$, where K_0 is the solution of Riccati equation, which is given as follows:

$$K_k = 1 + K_{k+1}/(1 + K_{k+1}), \qquad K_{N_{\text{dim}}} = 1 \tag{7}$$

In this case, two values of design variables N_{dim} are set to 10 and 30. The problem computation is performed with a population size N_{popsize} of 30. Figures 3a and 3b plot the convergence histories of the objective function for the four GAs for $N_{\text{dim}} = 10$ and 30. The proposed intelligent GA is shown to converge quickly and, furthermore, achieved a better minimum than the other three GAs. The final minima for the proposed intelligent GA, Taguchi-GA, micro-GA, and traditional GA are 161.8630, 161.8909, 161.8933, and 163.3866, respectively, after 5000 generations. Equation (6) indicates that the analytical solution is 161.8034. As N_{dim} increases to 30, the final minima for the proposed intelligent GA, Taguchi-GA, micro-GA, and traditional GA are 163.9794, 176.8140, 170.4883, and 301.020 after 20,000 generations. These four case computations demonstrate that the characteristics of fast convergence and high accuracy provide the present algorithm with high potential and a capacity for optimizing practical, complex engineering problems.

Profile Fitting of a High-Lift LS(1)-0417 Model Airfoil

A profile fitting for a high-lift LS(1)-0417 modified airfoil is presented for validating the presented intelligent GA. The airfoil coordinates, reported in Ref. 23, with 47 points on the upper and lower surfaces, are specified as the target points. Additionally, a NACA-0012 airfoil with 129 points distributed along the lower and upper surfaces is chosen as the initial profile. The objective function and the range of the design variables are

$$\text{minimize} \qquad \sqrt{\frac{1}{2n}\sum_{k=1}^{2n}(\boldsymbol{y}_k - \boldsymbol{y}_{\text{target}})^2}$$

$$\text{subject to} \qquad -0.1 \le x_i \le 0.1 \tag{8}$$

Here, n denotes the number of the target airfoil on the upper or lower surfaces, and the parameter x_i represents the design variable. In this case, $n = 47$. This work proposes polynomial shape functions for reducing the number of design variables. The new geometry coordinates of an airfoil are constructed by a linear superposition from the baseline airfoil coordinates and the geometry perturbations. The nondimensional coordinates of $\boldsymbol{y}$ for a given airfoil profile are specified as follows:

$$\bar{y}(\bar{x}) = \bar{y}_0 + \sum_{i=1}^{M} x_i f_i(\boldsymbol{x}) \tag{9}$$

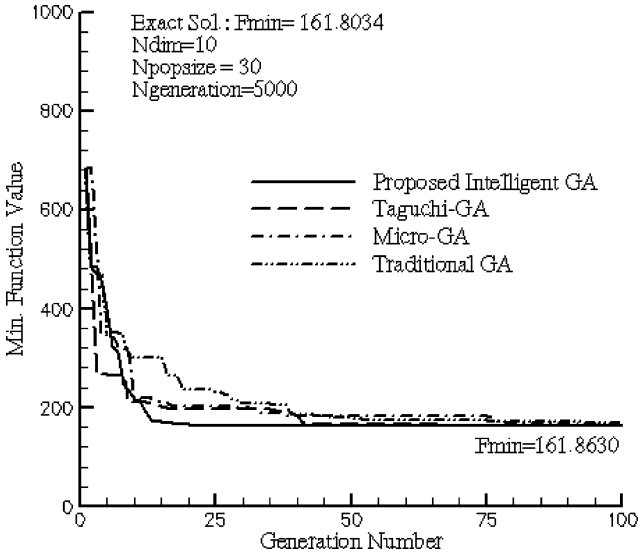

Fig. 3 Convergence histories and optimal solutions obtained with the traditional GA, micro-GA, Taguchi-GA, and proposed intelligent GA to solve the nonlinear dynamic control function with a) $N_{\text{dim}} = 10$ and b) $N_{\text{dim}} = 30$.

The symbols $\bar{x}$ and $\bar{y}_0$ represent the base airfoil coordinate along the x and y directions. The shape functions with M curves, with a total of 11 curves used in this investigation, are the combinations of the exponential and sinusoidal functions for perturbing the airfoil shape. The shape functions are expressed as follows:

$$f_1(\bar{x}) = \bar{x}^{0.25}(1-\bar{x})e^{-20x}$$

$$f_k(\bar{x}) = \sin^3\left(\pi \bar{x}^{e(k)}\right), \qquad k = 2, 3, 4, 5, 6$$

$$e(k) = [\ell n(0.5)/\ell n(\delta_k)], \qquad \delta_k = 0.1, 0.2, 0.3, 0.4, 0.5 \tag{10}$$

Additionally, the function forms for f_7–f_{11} are set as the mirrors of f_5–f_1 around the position $\bar{x} = 0.5$. The maximum value of each function occurs at $\bar{x} = \delta_k$. Notably, both functions f_1 and f_{11} dominant the variations of the contour near the leading and trailing edges of the airfoil. Accordingly, the total number of the design variable equals 22 when the shape functions are used on the upper and lower surfaces. That is, the GA sets N_{dim} as 22. The shape functions enable changes in both airfoil thickness and camber. When the GA

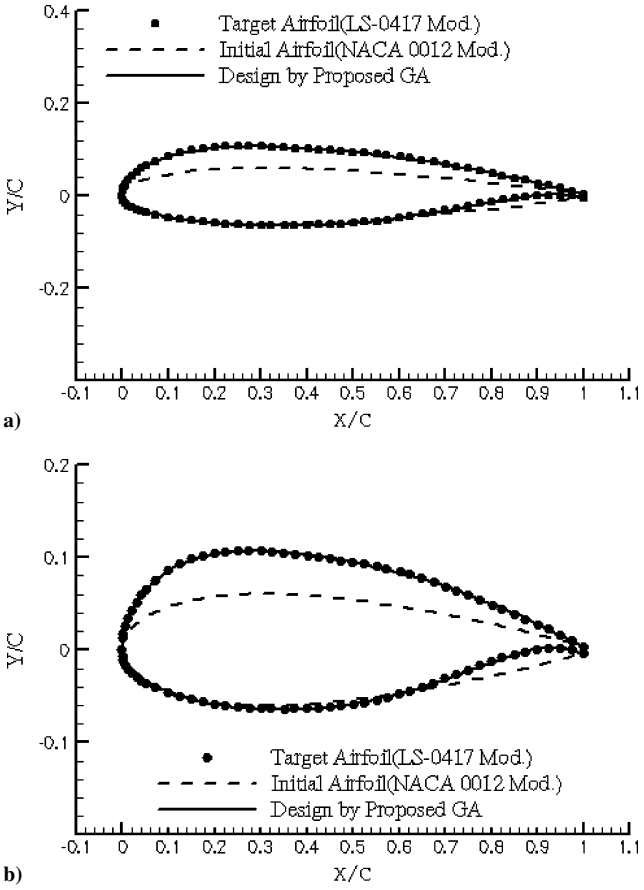

Fig. 4 Designed contour of high-lift LS(1)-0417 Model airfoil with a) normal and b) enlarged scales.

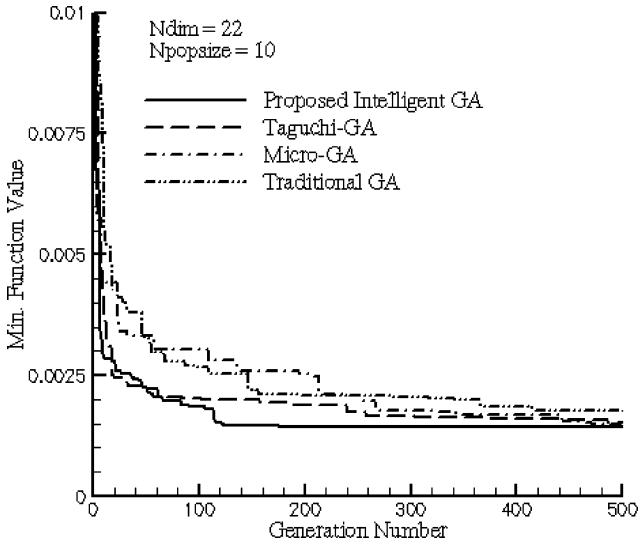

Fig. 5 Convergence histories and optimal solutions obtained with the traditional GA, micro-GA, Taguchi-GA, and proposed intelligent GA to design the contour of high-lift LS(1)-0417 modified airfoil.

is used to achieve the fitting curves, the designed airfoil shape for the LS(1)-0417 modified airfoil is presented with two scale plots. Figures 4a and 4b show the fitting airfoil plotted with normal and enlarged scales, respectively. In Figs. 4a and 4b, the circle symbols represent the target airfoil coordinates. The computational results show a good fit on the airfoil profile by the use of the presented intelligent GA. Moreover, Fig. 5 shows the convergence histories for the four GAs, and reveals that the present GA outperforms the others in terms of convergence rate and numerical accuracy. The minimum value of the objective function with the proposed GA is

0.00077 and is lower than the other three results obtained by the classical GA, micro-GA, and Taguchi-GA.

Aerodynamic Optimization of Airplanes

The presented intelligent GA is further applied to investigate the complex aerodynamic optimizations of two airplanes. One airplane is an advanced defense airplane, whereas the other is an F-16A fighter. When the Mach number of flight speed for an airplane approaches one, a high gradient drag rise always occurs in association due to the shock waves acting on the surfaces of the fuselage, wing, and tail. Therefore, the high drag force should be reduced as low as possible through an optimal aerodynamic design to improve flight performance at supersonic speeds. Because the wing planform design is the key element relative to the flight performance, the present study chooses the swept-back angle Λ_{LE}, aspect ratio AR, and taper ratio λ of the wing as the design variables for the redesign of the wing planform. The fuselage and tails are maintained as in the original. In the computations, the reference wing and exposed wing areas are set to be constant and identical to the original wing area of the airplane. Moreover, the exposed wing area is also set to equal the original configuration. This work uses an efficient drag estimation program to calculate the drag force through the subsonic to supersonic regimes. Moreover, this work employs a vortex strip code to analyze the aerodynamic force and moment for an airplane at subsonic and supersonic speeds. Combining the two aerodynamic programs with the proposed intelligent GA can achieve workable computing for complex airplane optimizations. Figure 6 is a detailed flowchart.

The advanced defense airplane is the first configuration requiring optimization. The range of design variables of Λ_{LE}, AR, and λ is set to [30, 50], [2, 4], and [0.2, 0.3], respectively. Figure 7 shows the convergence histories obtained with the four GAs. Clearly, the proposed intelligent GA outperforms the other three GAs because it required only a few generation numbers to achieve the optimal function value. Figures 8a and 8b show the original and optimal wing planforms. The design variables (Λ_{LE}, AR, and λ) for the original and optimal wing planforms are (31.44 deg, 3.063, 0.2368) and (33.77 deg, 3.25, 0.2002). Figure 9 shows that the results obtained by the four GAs are almost identical. As studied in the first multimodal function, given a small number of design variables, for example, 2–5, the GAs always reach good results. In this case, an approximately 2.18% reduction in the average drag coefficient is observed in the supersonic region. This reduction represents a large improvement of flight performance in the high-speed flight owing to the relatively high dynamic pressure in this speed regime. This work implies that

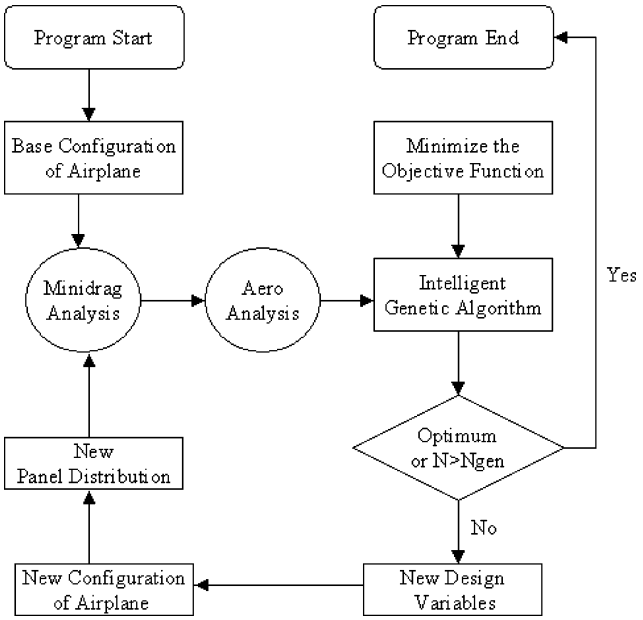

Fig. 6 Flowchart for otimizing aerodynamic design of an airplane.

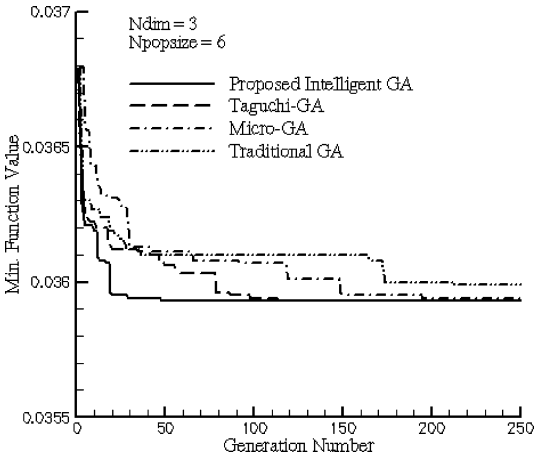

Fig. 7 Convergence histories and optimal objective values obtained with the traditional GA, micro-GA, Taguchi-GA, and proposed intelligent GA to redesign the wing planform of the advanced defense airplane.

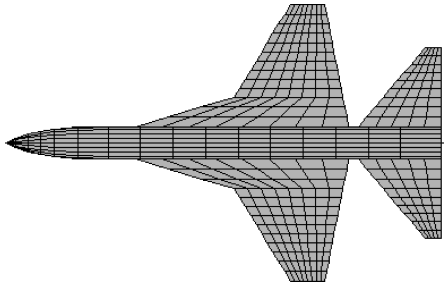

a) Original: $\Lambda_{LE} = 31.44$ deg, AR = 3.063, $\lambda = 0.2368$, $S_{ref} = 261$ ft^2, and $b = 28.28$ ft

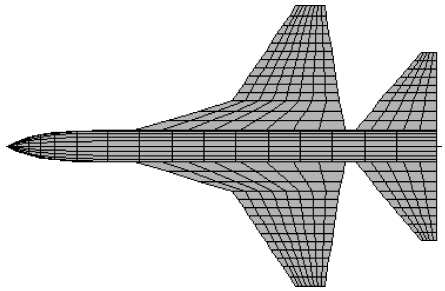

b) Redesigned: $\Lambda_{LE} = 33.77$ deg, AR = 3.25, $\lambda = 0.2002$, $S_{ref} = 261$ ft^2, and $b = 29.125$ ft

Fig. 8 Wing planforms of the advanced defense airplane.

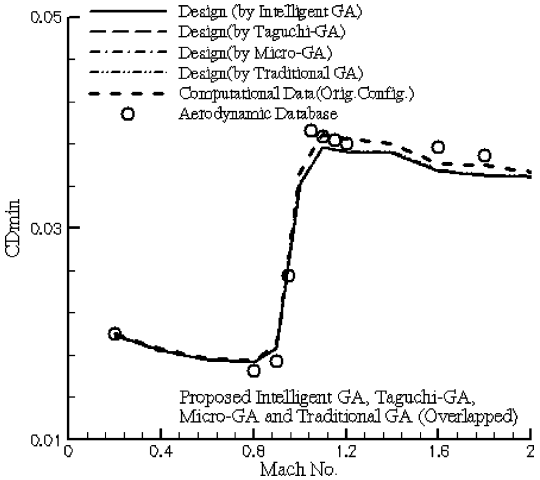

Fig. 9 Comparison of drag distributions obtained with the traditional GA, micro-GA, Taguchi-GA, and proposed intelligent GA to redesign the wing planform of the advanced defense airplane.

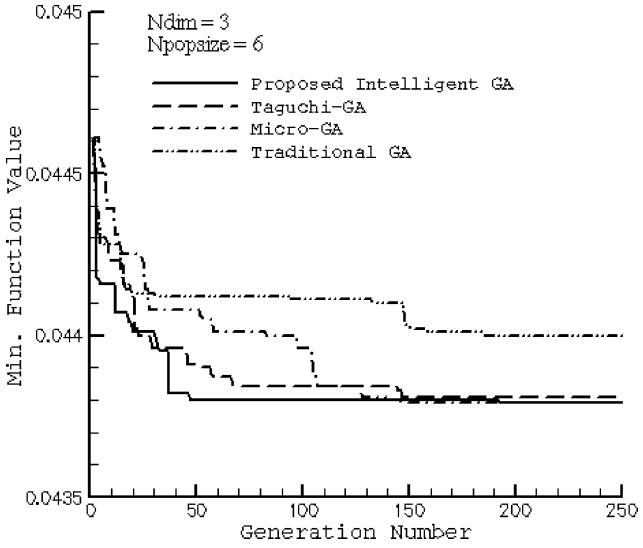

Fig. 10 Convergence histories and optimal objective values obtained with the traditional GA, micro-GA, Taguchi-GA, and proposed intelligent GA to redesign the wing planform of the F-16A fighter.

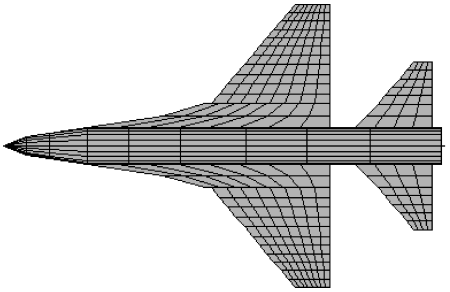

a) Original: $\Lambda_{LE} = 40$ deg, $AR = 3$, $\lambda = 0.2275$, $S_{ref} = 300$ ft^2, and $b = 30$ ft

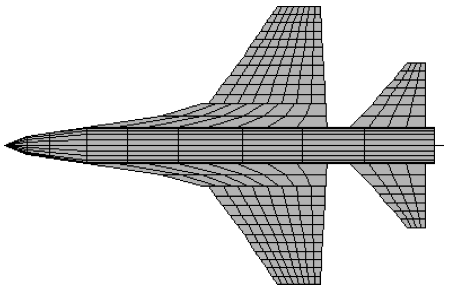

b) Redesigned: $\Lambda_{LE} = 36.89$ deg, $AR = 2.75$, $\lambda = 0.2854$, $S_{ref} = 300$ ft^2, and $b = 28.724$ ft

Fig. 11 Wing planforms of the F-16A fighter.

less engine power is required in the supersonic cruise when the fighter uses the redesigned wing planform.

Moreover, this work optimizes the aerodynamics of an F-16A fighter, originally designed by General Dynamics (GD) Corp., by the four GAs. This fighter has excellent aerodynamic performance in terms of flight maneuverability. The original geometric parameters for the Λ_{LE}, AR, and λ are 40 deg, 3.0, and 0.2275, respectively. Figure 10 presents the convergence histories obtained by the four GAs. Figure 10 shows an excellent result for the proposed intelligent GA. The convergence rate that uses the traditional GA is relatively slow in this case. Figures 11a and 11b show that the optimal geometric parameters for the Λ_{LE}, AR, and λ are 36.89 deg, 2.75, and 0.2854. The redesigned wing planform shortens the span and increases the taper ratio. Figure 12 shows the drag force distribution for the original and redesign configurations from subsonic to supersonic speed. The results of the four GAs are also almost identical to those in the preceding case. In the case with the four GAs, a reduction of around

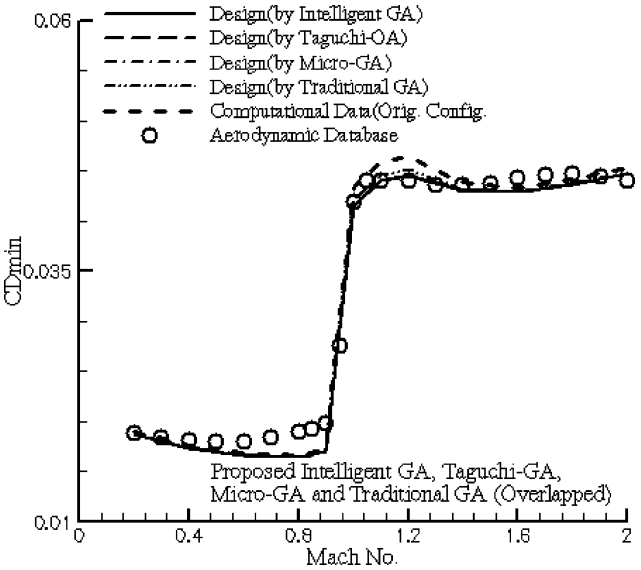

Fig. 12 Comparison of drag distributions obtained with the traditional GA, micro-GA, Taguchi-GA, and proposed intelligent GA to redesign the wing planform of the F-16A fighter.

1.86% in average drag coefficient is measured in the supersonic region.

Conclusions

This work proposed a new intelligent GA that incorporates the FFD in the crossover operator for intelligent determination of the best genes for children produced by the mating of a pair of parents. However, the crossover operation in the traditional GA is implemented by randomly exchanging genes from parents. Therefore, the proposed intelligent crossover operation effectively enhances the evolutionary efficiency of the traditional GA. This work listed the pseudocode and numerical procedure for FFD step-by-step for constructing the intelligent GA. The methodology of the traditional GA presented here uses tournament selection, uniform crossover, jump mutation, and an elitist strategy. The main difference between the micro-GA and traditional GA lies in the mutation operator. Moreover, this work also developed the Taguchi-GA, which employs the Taguchi OAs rather than the FFD, for constructing another crossover operator. Additionally, the present intelligent GA employs the strategy of two children per pair of parents and achieves high computational efficiency for reducing the CPU by 50% for offspring generation. Several test cases, including two multimodal functions, a nonlinear dynamic control function, and a profile fitting of a high-lift airfoil, are performed with the traditional GA, micro-GA, Taguchi-GA, and the proposed intelligent GA to evaluate the algorithm capacity and efficiency. The computational results show that the proposed intelligent GA outperforms the traditional GA, micro-GA, and Taguchi-GA. This study also applies the four GAs for the aerodynamic optimization of two advanced airplanes. One of the subject airplanes is the advanced defense airplane, whereas the other is the F-16A fighter. The total drag reduction achieved for the defense aircraft and the F-16A fighter was 2.18 and 1.86%, respectively, at supersonic speeds. Based on the numerical evaluations, the proposed intelligent GA performs well in terms of convergence and optimal solution. The evaluations also demonstrated that the presented GA is robust for optimizing complex aerodynamic problems.

References

[1]Coley, D. A., *An Introduction to Genetic Algorithms for Scientists and Engineering,* reprinted ed., World Scientific, Singapore, 2001, Chaps. 1 and 6.

[2]Holland, J. H., *Adaptation in Natural and Artificial Systems*, 1st ed., Univ. of Michigan Press, Ann Arbor, MI, 1975, Chap. 6.

[3]Goldberg, D. E., *Genetic Algorithms in Search, Optimization, and Machine Learning*, 1st ed., Addison–Wesley, Reading, MA, 1989, pp. 10–19, 343–349.

[4]Vicini, A., and Quagliarella, D., "Airfoil and Wing Design Through Hybrid Optimization Strategy," *AIAA Journal*, Vol. 37, No. 9, 1999, pp. 634–641.

[5]Yen, J., Liao, J. C., Lee, B., and Randolph, D., "A Hybrid Approach to Modeling Metabolic Systems Using a Genetic Algorithm and Simplex Method," *IEEE Transactions on Systems, Man and Cybernetics*, Vol. 28, Pt. B, No. 2, 1998, pp. 173–191.

[6]Jeong, I. K., and Lee, J. J., "Adaptive Simulated Annealing Genetic Algorithm for System Identification," *Engineering Application of Artificial Intelligence*, Vol. 9, No. 5, 1996, pp. 523–532.

[7]Murata, T., Ishibuchi, H., and Tanaka, H., "Genetic Algorithms for Flowshop Scheduling Problems," *Computers Industry Engineering*, Vol. 30, No. 4, 1996, pp. 1061–1071.

[8]Liaw, C. F., "A Hybrid Genetic Algorithm for Open Shop Scheduling Problem," *European Journal of Operational Research*, Vol. 124, No. 1, 2000, pp. 28–42.

[9]Ho, S. Y., Shu, L. S., and Chen, H. M., "Intelligent Genetic Algorithm with a New Intelligent Crossover Using Orthogonal Array," *Proceedings of 1999 Genetic and Evolutionary Computation Conference*, Vol. 1, 1999, pp. 289–296.

[10]Bhote, K. R., *World Class Quality: Using Design of Experiments to Make It Happen*, 1st ed., American Management Association, New York, 1991, Chap. 5.

[11]Ross, P. J., *Taguchi Techniques for Quality Engineering*, 2nd ed., McGraw–Hill, New York, 1996, Chap. 7.

[12]Shainin, D., and Shainin, P., "Better Than Taguchi Orthogonal Tables," *Quality and Reliability Engineering International*, Vol. 4, No. 2, 1988, 143–149.

[13]Goldberg, D. E., and Deb, K., "A Comparitive Analysis of Selection Schemes Used in Genetic Algorithms," *Foundations of Genetic Algorithms*, edited by G. J. E. Rawlins, Morgan Kaufmann, San Mateo, CA, 1991, pp. 69–93.

[14]Krishnakumar, K., "Micro-Genetic Algorithms for Stationary and Non-Stationary Function Optimization," *SPIE's Intelligent Control and Adaptive Systems*, Society of Photo-Optical Instrumentation Engineers, Bellingham, WA, 1989, pp. 289–296.

[15]Yang, G., Reinstein, L. E., Pai, S., Xu, Z., and Carroll, D. L., "A New Genetic Algorithm Technique in Optimization of Permanent Prostate Implants," *Medical Physics*, Vol. 25, No. 12, 1998, pp. 2308–2315.

[16]Hicks, R. M., and Henne, P. A., "Wing Design by Numerical Optimization," *Journal of Aircraft*, Vol. 15, No. 7, 1978, pp. 407–412.

[17]Vanderplaats, G. N., "Efficient Algorithm for Numerical Airfoil Optimization." *Journal of Aircraft*, Vol. 16, No. 12, 1979, pp. 842–847.

[18]Oyama, A., Obayashi, S., and Nakahashi, K., "Euler/Navier–Stokes Optimization of Supersonic Wing Design Based on Evolutionary Algorithm," *AIAA Journal*, Vol. 37, No. 10, 1999, pp. 1327–1328.

[19]Nemec, M., Zingg, D. W., and Pulliam, T. H., "Multipoint and Multi-objective Aerodynamic Shape Optimization," *AIAA Journal*, Vol. 42, No. 6, 2004, pp. 1057–1065.

[20]Ahmed, Q., Krishnakumar, K., and Neidhoefer, J., "Applications of Evolutionary Algorithms to Aerospace Problems-A Survey," *Computational Methods in Applied Sciences' 96*, Wiley, London, 1996, pp. 236–242.

[21]Goldberg, D. E., and Richardson, J., "Genetic Algorithms with Sharing for Multimodal Function Optimization," *Genetic Algorithms and Their Applications: Proceedings of the Second International Conference on Genetic Algorithms*, 1987, pp. 41–49.

[22]Michalewicz, Z., *Genetic Algorithms + Data Structures = Evolution Programs*, 3rd ed., Springer-Verlag, Berlin, 1999, p. 100.

[23]McGhee, R. J., and Beasley, W. D., "Wind Tunnel Results for a Modified 17-Percent-Thick Low-Speed Airfoil Section," NASA TP-1919, Nov. 1981.

E. Livne
Associate Editor